EPJ Web of Conferences **274**, 03011 (2022) https://doi.org/10.1051/epjconf/202227403011
*XV$^{th}$ Quark Confinement and the Hadron Spectrum*

# Glueballs in Radiative $J/\psi$ Decays

*Eberhard* Klempt[1,*]

[1]HISKP der Rheinischen Friedrich-Wilhelms-Universität, Nußallee 14-16, 53115 Bonn, Germany

**Abstract.** The scalar glueball is observed in a coupled-channel analysis of the $S$-wave amplitude from BESIII data on radiative $J/\psi$ decays and further data. Ten scalar isoscalar resonances were required to fit the data. Five of them were interpreted as mainly-singlet, five as mainly-octet resonances in SU(3). The yield of resonances showed a striking peak with properties expected from a scalar glueball:

- $G_0(1865)$ is produced abundantly in radiative $J/\psi$ decays above a very low background. Its mass is $1\sigma$ compatible with the mass calculated in unquenched lattice QCD, and the yield is $1.6\sigma$ compatible with the yield calculated in lattice QCD.
- The decay analysis of the scalar isoscalar mesons shows that the assignment of mesons to mainly-octet and mainly-singlet states is correct. Even the production of mainly-octet scalar mesons - which should be forbidden in radiative $J/\psi$ decays - peaks at 1865 MeV. The decay analysis requires a small glueball content in the flavor wave function of several scalar resonances. The glueball content as a function of the mass shows a peak compatible with the peak in the yield of scalar isoscalar mesons. The sum of the fractional glueball contributions is compatible with one.
- In the reaction $B_s \to J/\psi + K^+K^-$ reported by the LHCb collaboration, a primary $s\bar{s}$ couples to mesons having a strong coupling to $K^+K^-$. Two peaks in the $K^+K^-$ mass spectrum are seen due to $\phi(1020)$ and $f_2'(1525)$, but there is little evidence for the $f_0(1710)$ or other high-mass scalar mesons coupling strongly to $K\bar{K}$. High-mass scalar mesons are strongly produced by two initial-state gluons but not by an $s\bar{s}$ pair in the initial state. They must have sizable glueball fractions!
- The $D$ wave amplitude in the BESIII data on radiative $J/\psi$ decays reveales a high-mass structure which can be described by a single Breit-Wigner or by the sum of three $\phi\phi$ resonances interpreted as tensor glueballs a long time ago. The structure - and further tensor resonances observed in radiative $J/\psi$ decays - are tentatively interpreted as tensor glueball.
- In $J/\psi$ decays into $\gamma\pi^0\pi^0\eta'$ several resonances are reported. The possibility is discussed that the pseudoscalar glueball might be hidden in these data.

*e-mail: Klempt@hiskp.uni-bonn.de

## 1 Introduction

The self-interaction between gluons leads to the prediction of glueballs. Their masses are calculated by discretization of QCD on a lattice or in approximate solutions of QCD. A large number of glueball is predicted with the scalar glueball as ground state, followed in mass by a tensor and a pseudoscalar glueball. Typical masses of the lowest-mass glueballs are shown below:

| | | | | |
|---|---|---|---|---|
| $0^{++}$ | 1710±50± 80 MeV [1] | 1850±130 MeV [2] | 1980 MeV [3] | 1920 MeV [4] |
| $2^{++}$ | 2390±30±120 MeV [1] | 2610±180 MeV[2] | 2420 MeV [3] | 2371 MeV [4] |
| $0^{-+}$ | 2560±35±120 MeV [1] | 2580±180 MeV [2] | 2220 MeV [3] | |

The widths are essentially undetermined. The yields of glueballs have been calculated for the process $J/\psi \to \gamma G$. The yields are surprisingly high: the largest radiative yield of a meson, $J/\psi \to \gamma\eta'$, is $(5.25\pm0.07)\cdot10^{-3}$. The yield of the tensor glueball is expected to be larger by a factor 2! The pseudoscalar yield is given for two glueball masses.

| | | | | | |
|---|---|---|---|---|---|
| $BR_{J/\psi\to\gamma G_{0^{++}}}$(TH) | $=$ | $(3.8 \pm 0.9)$ | $\cdot10^{-3}$ | | [5] |
| | $\approx$ | 3 | $\cdot10^{-3}$ | | [6] |
| $BR_{J/\psi\to\gamma G_{2^{++}}}(TH)$ | $=$ | $(11 \pm 2)$ | $\cdot10^{-3}$ | | [7] |
| $BR_{J/\psi\to\gamma G_{0^{-+}}}(TH)$ | $=$ | $(0.231 \pm 0.080)$ | $\cdot10^{-3}$ | M=2395 MeV | [8] |
| | $=$ | $(0.107 \pm 0.037)$ | $\cdot10^{-3}$ | M=2560 MeV | [8] |

The scalar glueball is often supposed to intrude the spectrum of scalar mesons and to mix with them. So far, authors have assumed that the three scalar mesons $f_0(1370)$, $f_0(1500)$, $f_0(1710)$ contain the $1^3P_0$ $n\bar{n}$ and $s\bar{s}$ scalar mesons and the glueball of lowest mass. Since only two scalar isoscalar mesons in one nonet are expected, one of the three states seems to be supernumerous, hence a glueball must have entered. The decay modes of all three mesons are incompatible with one beeing a pure glueball, hence these three mesons are supposed to mix

$$\begin{array}{c} f_0(1370) \\ f_0(1500) \\ f_0(1710) \end{array} = \begin{pmatrix} x_{11} & x_{12} & x_{13} \\ x_{21} & x_{22} & x_{23} \\ x_{31} & x_{32} & x_{33} \end{pmatrix} \begin{array}{c} |n\bar{n}\rangle \\ |s\bar{s}\rangle \\ |gg\rangle \end{array}$$

where the mixing has to be determined from the decay (and the production) of the three mesons.

## 2 Data and coupled channel analysis

Radiative decays of $J/\psi$ mesons is the prime source to discover glueballs. $J/\psi$ mesons can convert into three gluons or into one photon and two gluons. These two gluons interact and should form glueballs – if glueballs exist. In Ref. [11] a coupled-channel analysis of a large number of data sets was reported. Of particular importance are

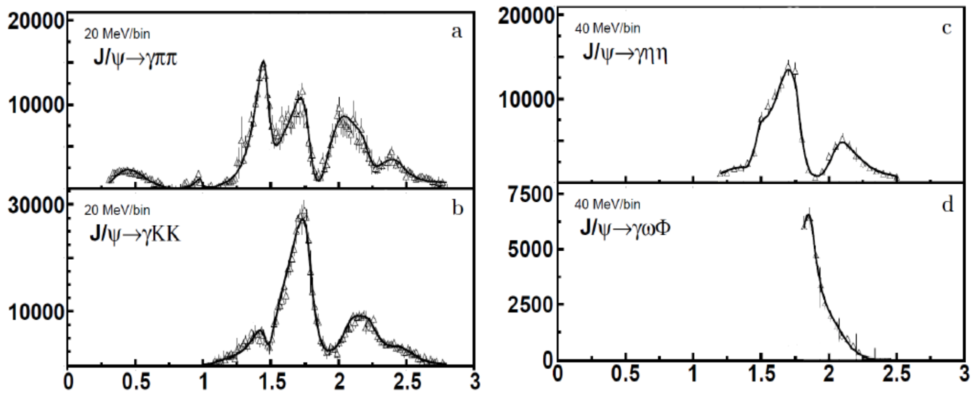


**Figure 1.** The scalar intensity in $J/\psi \to \gamma\pi^0\pi^0$ (a), $K_s^0 K_s^0$ (b), $\eta\eta$ (c) and to $\omega\phi$ (d) from Ref. [9, 10]. The curves represent the best fit [11].

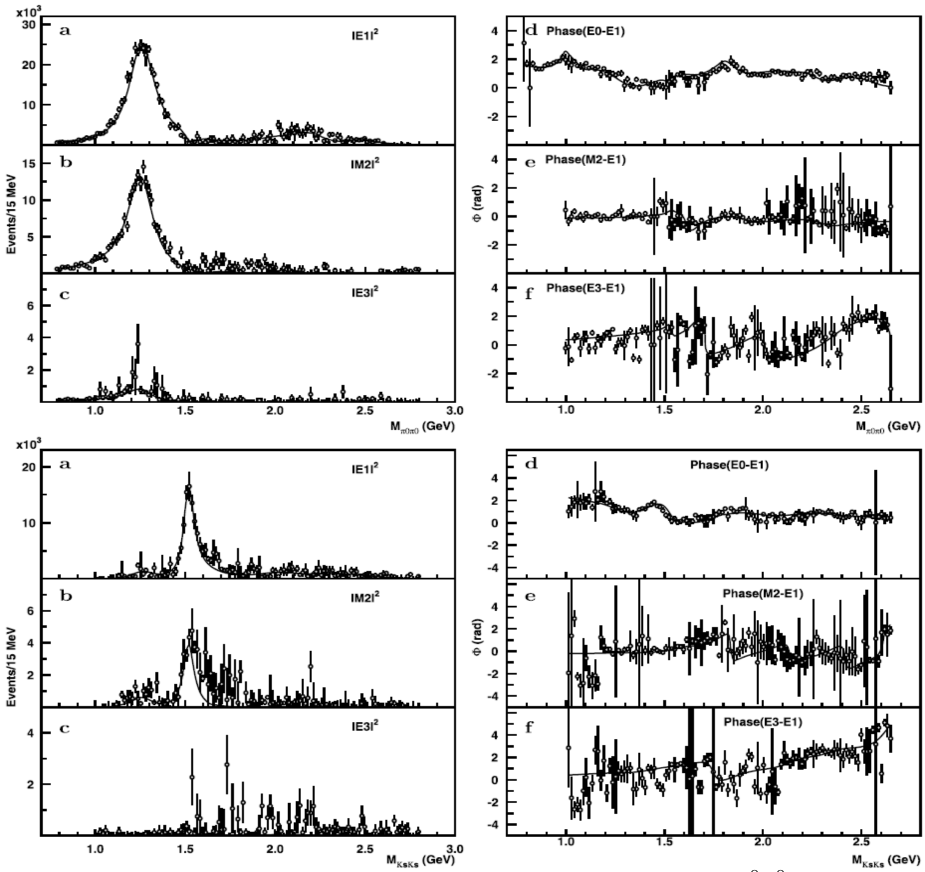


**Figure 2.** *D*-wave intensities and phases for radiative $J/\psi$ decays into $\pi^0\pi^0$ (top subfigures) and $K_s K_s$ (bottom subfigures) from Ref. [9, 10]. The subfigures show the $E1$ (a), $M2$ (b) and $E3$ (c) squared amplitudes and the phase differences between the $E0$ and $E1$ (d) amplitudes, the $M2$ and $E1$ (e) amplitudes, and the $E3$ and $E1$ (f) amplitudes as functions of the meson-meson invariant mass. The phase of the $E0$ amplitude is set to zero. The curves represent the best fit [12].

https://doi.org/10.1051/epjconf/202227403011

the results from an amplitude analysis of $J/\psi \to \gamma\pi^0\pi^0$ [9] and $K_s^0 K_s^0$ [10], supported by BESIII data on $J/\psi \to \eta\eta$ and to $\omega\phi$. The CERN-Munich data on $\pi\pi$ elastic scattering with the $\pi\pi$ $S$-wave are mandatory to get the right solution. The GAMS data, in particular those on $\pi^0\pi^0$ production from high-energy $\pi N$ scattering force the solution above 1.6 GeV. The data on $K_{e4}$ decays fix the low-mass part of the amplitude. Furthermore, 15 Dalitzplot from $p\bar{p}$ annihilation at rest are included in the analysis as well as BNL data on $\pi\pi \to K_s^0 K_s^0$ and further GAMS data. References to the data can be found in Ref. [11].

Figure 1 shows invariant mass distributions of the BESIII data assigned to the $S$-wave, Figure 2 (left) the $D$-wave for $\pi^0\pi^0$ and $K_s^0 K_s^0$. The $D$ wave can be excited by three electromagnetic amplitudes, $E1, M2$, and $E3$, where the $E1$ amplitude is the most significant one. These three amplitudes and relative phases are shown in Fig. 2 (right).

## 3 The scalar glueball

From the fit, existence and properties are scalar mesons are deduced. Figure 3 shows their squared masses as a function of a consecutive number. The mesons are grouped pairwise. The higher-mass states are interpreted as octet states in SU3, the lower-mass states as singlet states. These assignments are verified in an analysis of their decays discussed below. The scalar glueball is identified by three different methods.

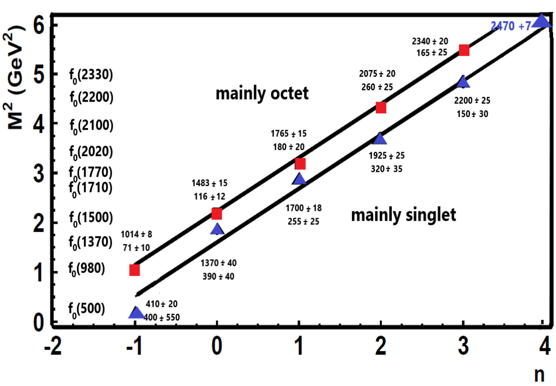


**Figure 3.** The square masses of scalar mesons as a function of a consecutive number [11]. The numbering starts with -1 since $f_0(500)$ and $f_0(980)$ may not belong to the series. Masses and widths are given in small numbers. The SU3 assignment is discussed in the text. The meson at 2470 MeV was seen by BESIII in $J/\psi \to \gamma\eta'\eta'$ decays [13]. Due to its decay it likely belongs to the mainly singlet states.

*The scalar glueball from the yield in radiative $J/\psi$ decays:*

First, the total radiative yield of scalar mesons is plotted as a function of their mass for both mainly-octet and mainly-singlet mesons (see Fig. 4, left). Radiative production of mainly-octet mesons should be suppressed: two gluons cannot convert into an octet meson. The fact that mainly-octet mesons are produced at the same rate as mainly-singlet mesons can only be explained when these mesons are dominantly produced via their glueball component. The total yield is derived from the fit described here and from known radiative decay branching ratios of the $J/\psi$ meson.

A fit to the yield shown in Fig. 4 (left) with a Breit-Wigner function returns mass, width and yield:

$$M - \frac{1}{2}\Gamma = (1865 \pm 25\,^{+10}_{-30}) - i(185 \pm 25\,^{+15}_{-10})\,\text{MeV}, \quad Y = (5.8 \pm 1.0)\,10^{-3}.$$

 https://doi.org/10.1051/epjconf/202227403011

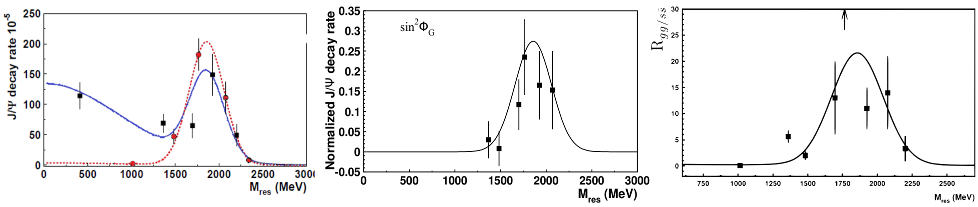


**Figure 4.** The scalar glueball is identified by three methods: the radiative yield of $J/\psi$ decays into scalar singlet and isoscalar octet mesons peaks at 1.865 MeV (left); the glueball component in the mesonic wave function of scalar mesons peaks at the same mass (center, [14]); the ratio of the yields of scalar mesons in radiative $J/\psi$ decays and in $B_s \to J/\psi +$ scalar mesons peaks as well (right).

*The scalar glueball from the decays of scalar mesons:*

The second method exploits the decay modes of the scalar mesons [14]. The decay modes depend on the mixing angle of the singlet and the octet isoscalar mesons belonging to the same nonet. Figure 5 shows the squared coupling constants for meson decays into two pseudoscalar mesons as a function of the mixing angle.

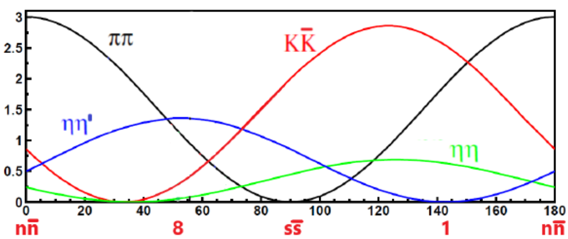


**Figure 5.** Squared coupling constants $\gamma_\alpha$ for meson decays into a pair $\alpha$ of pseudoscalar mesons [14]. For the mixing angle 90°, e.g., the meson is a pure $s\bar{s}$ state and there are no $\pi\pi$ decays.

The wave function of a meson can be decomposed into its $n\bar{n}$, $s\bar{s}$ and glueball component $G$, where $\varphi_{\rm n}^{\rm s}$ is the scalar mixing angle in nonet $n$, $\phi_{\rm nL}^{G}$ and $\phi_{\rm nH}^{G}$ are the meson-glueball mixing angles of the low-mass state L and of the high-mass state H in the nth nonet. $\sin^2\phi_{\rm nH}^{G}$ and $\sin^2\phi_{\rm nL}^{G}$ are the glueball contents of the two mesons.

$$f_0^{\rm nH}(xxx) = (n\bar{n}\cos\varphi_{\rm n}^{\rm s} - s\bar{s}\sin\varphi_{\rm n}^{\rm s})\cos\phi_{\rm nH}^{G} + G\sin\phi_{\rm nH}^{G}$$

$$f_0^{\rm nL}(xxx) = (n\bar{n}\sin\varphi_{\rm n}^{\rm s} + s\bar{s}\cos\varphi_{\rm n}^{\rm s})\cos\phi_{\rm nL}^{G} + G\sin\phi_{\rm nL}^{G}$$

The coupling of a meson to the final state $\alpha$ can be written as $g_\alpha^{\rm n} = c_{\rm n}\gamma_\alpha^q + c_G\gamma_\alpha^G$. Here, the $q\bar{q}$ and the glueball components of a scalar meson couple with the SU(3) structure constants $\gamma_\alpha$ and with a decay coupling constant $c_n$ or $c_G$ to the final states $\alpha$. A fit to the decay branching ratios yields the glueball fractions of the scalar mesons [14]. These are shown in Fig. 3. The glueball fractions derived from the decay of scalar mesons into two pseudoscalar mesons shows a peak with a shape that is fully compatible with the peak in the yield of scalar mesons in radiative $J/\psi$ decays. In $f_0(1370)$-$f_0(1500)$-$f_0(1710)$ mixing scenarios, it is imposed that the full glueball is distributed over the three mesons. Here, the sum of the glueball fractions is determined to 0.78±0.18. The information of the highest-mass scalar meson is insufficient to determine a glueball content. Since this part is missing, nearly the full glueball is covered and distributed over the mesons observed in radiative $J/\psi$ decays.

*The scalar glueball from a comparison with $B_s \to J/\psi f_0$ and $J/\psi \to \gamma f_0$:*

In $J/\psi$ radiative decays, a photon is emitted and two gluons are created which convert into an observable meson. In $B^0$ and $B_s$ decays into a $J/\psi$ meson recoiling against a $\pi^+\pi^-$ or $K^+K^-$ pair, a primary $d\bar{d}$ or $s\bar{s}$ pair is produced which form a meson (see Fig. 6). The LHCb collaboration studied this process and the mixing of $B^0$

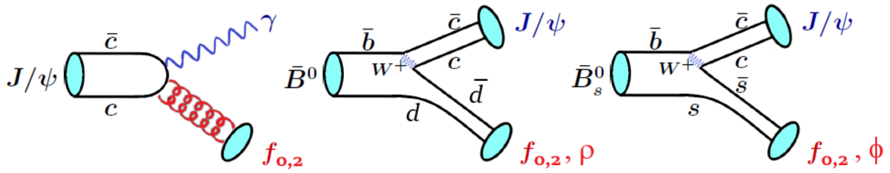


**Figure 6.** Scalar meson production in $B^0 \to J/\psi\, f_0$, $B_s \to J/\psi\, f_0$, $J/\psi \to \gamma f_0$.

and $B_s$ mesons with their antiparticles and determined the decay-time-dependent CP asymmetry. The collaboration also presented spherical harmonic moments and their dependence of the $\pi^+\pi^-$ or $K^+K^-$ invariant mass and interpreted these results in terms of contributing resonances. These data were included in the coupled-channel analysis of Ref. [11]. The data and the fit are shown in Fig. 7.

The scalar intensity is surprisingly small, in particular above 1600 MeV. The $f_0(1710)/f_0(1770)$ complex that is seen so strongly in $J/\psi \to \gamma f_0(1710)/f_0(1770) \to \gamma K\bar{K}$ is nearly absent when a primary $s\bar{s}$ pair is present at the same invariant mass and under similar kinematical conditions. The wave function of high-mass mesons obviously have little overlap with a local $s\bar{s}$ pair. However, a small glueball fraction in a mesonic wave function enhances the chance to produce this meson in radiative $J/\psi$ decays.

In Fig. 2 (right), the ratio of frequencies for scalar meson production in $J/\psi \to \gamma f_0$ and $B_s \to J/\psi\, f_0$ decays is shown as a function of the scalar meson mass. The distribution is compared to the Breit-Wigner shape determined from the yield distribution in Fig. 4. The ratio is fully compatible with the Breit-Wigner fit, even though with limited statical accuracy.

*The scalar glueball summary:*

The scalar glueball is identified from the yield of scalar mesons in radiative $J/\psi$ decays, from the decay-mode analysis of scalar mesons, and from a comparison of the yield of scalar mesons in $J/\psi \to \gamma f_0$ and $B_s \to J/\psi\, f_0$ decays.

## 4 Evidence for the tensor glueball

Figure 2 shows large signals due to $f_2(1270) \to \pi\pi$ and $f_2'(1525) \to K\bar{K}$. In the $\pi\pi$ invariant mass spectrum a further enhancement is seen with mass, width and yield

$$M - \frac{1}{2}\Gamma = (2210 \pm 60) - i(180 \pm 60)\,\text{MeV}, \quad Y = (0.35 \pm 1.0)\,10^{-3},$$

where the yield is the sum of the $\pi\pi$ and $K\bar{K}$ contributions. Again, this peak is absent in $B^0$ and $B_s$ decays. Hence it is likely produced due to a small tensor-glueball component in the wave function. The yield is low even if all intensity reported from $J/\psi \to \gamma f_2$ decays above 1.8 GeV is added [12]. The peak can be fitted as sum of the three tensor resonances reported in the doubly OZI rule violating process $\pi^- p \to \phi\phi n$. The three states were proposed as one, two or three tensor glueballs [18].

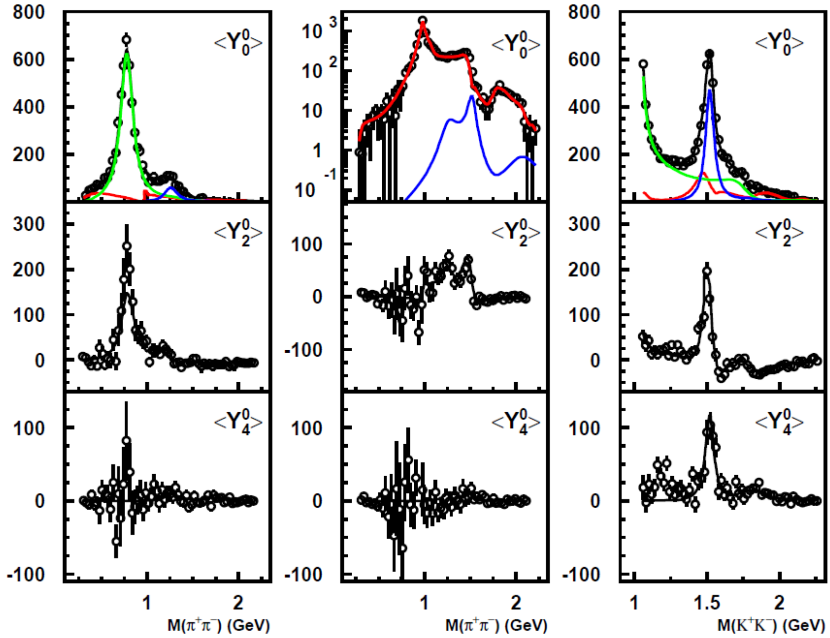


**Figure 7.** (Color online) The spherical harmonic moments $\cos\theta_{h\bar{h}}$ for $\bar{B}^0 \leftrightarrow B^0 \to J/\psi\pi^+\pi^-$ (left, [15]), $\bar{B}_s^0 \leftrightarrow B_s^0 \to J/\psi\pi^+\pi^-$ (center, [16]), and into $J/\psi\, K^+K^-$ (right, [17]). The points with error bars represent the LHCb data, the solid curve our fit. Partial waves with $L \geq 6$ and Odd partial waves are not included in the fit. The $S$-wave ($P$-wave, $D$-wave) contribution is shown as red (green, blue) curve.

## 5 How to find the pseudoscalar glueball

In the $\pi^+\pi^-\eta'$ invariant mass distribution observed in $J/\psi \to \pi^+\pi^-\eta'$, a series peaks is observed [19] (see inset of Fig. 8). We tentatively assume that they have pseudoscalar quantum numbers. Two linear trajectories can be drawn. The resonances above 2 GeV might be split: the $\eta' f_0(1500)$ isobar would be an octet-like state, $\eta' f_0(1370)$ a singlet-like state. The separation would require a cut in the $\pi\pi$ invariant mass into a region below and above 1480 MeV. Then, peaks at slightly different masses should be seen in the $\pi^+\pi^-\eta'$ invariant mass distribution. High-mass mesons of low spins are often suppressed in hadronic reactions. If they have a glueball component, their production in radiative $J/\psi$ decays could be significant. Hence I suggest that the pseudoscalar glueball may be wide and that at least all peaks above 2 GeV in Fig. 8a have a significant glueball fraction in their wave function.

## 6 Conclusions

Radiative $J/\psi$ decay have revealed the scalar glueball and show evidence for the tensor glueball. First traces of the pseudoscalar glueball may have shown up as well. The high statistics now available from BESIII and modern coupled-channel analyses have the chance to observed more decay modes and to improve our understanding of the glueball spectrum.

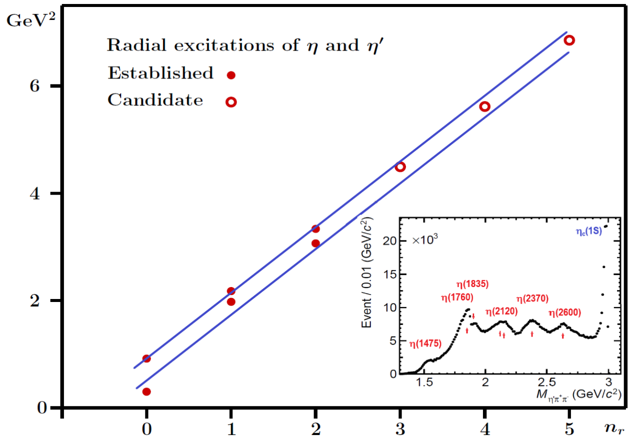


**Figure 8.** Left: Suggested $M^2$-versus-n plot of structures interpreted as pseudoscalar mesons. The data from Ref. [19]) are shown as inset.

*I would like to thank the organizer of this conference for the kind invitation to this interesting conference in such a beautiful place.*

## References

[1] C.J. Morningstar, M.J. Peardon, Phys. Rev. D **60**, 034509 (1999), hep-lat/9901004
[2] M.Q. Huber, C.S. Fischer, H. Sanchis-Alepuz, Eur. Phys. J. C **81**, 1083 (2021), [Erratum: Eur.Phys.J.C 82, 38 (2022)], 2110.09180
[3] A.P. Szczepaniak, E.S. Swanson, Phys. Lett. B **577**, 61 (2003), hep-ph/0308268
[4] M. Rinaldi, V. Vento, Phys. Rev. D **104**, 034016 (2021), 2101.02616
[5] L.C. Gui, Y. Chen, G. Li, C. Liu, Y.B. Liu, J.P. Ma, Y.B. Yang, J.B. Zhang (CLQCD), Phys. Rev. Lett. **110**, 021601 (2013), 1206.0125
[6] S. Narison, Nucl. Phys. B **509**, 312 (1998), hep-ph/9612457
[7] Y. Chen, L.C. Gui, G. Li, C. Liu, Y.B. Liu, J.P. Ma, Y.B. Yang, J.B. Zhang, PoS **LATTICE2013**, 435 (2014), 1402.3923
[8] L.C. Gui, J.M. Dong, Y. Chen, Y.B. Yang, Phys. Rev. D **100**, 054511 (2019), 1906.03666
[9] M. Ablikim et al. (BESIII), Phys. Rev. D **92**, 052003 (2015), [Erratum: Phys.Rev.D 93, 039906 (2016)], 1506.00546
[10] M. Ablikim et al. (BESIII), Phys. Rev. D **98**, 072003 (2018), 1808.06946
[11] A.V. Sarantsev, I. Denisenko, U. Thoma, E. Klempt, Phys. Lett. B **816**, 136227 (2021), 2103.09680
[12] E. Klempt, K.V. Nikonov, A.V. Sarantsev, I. Denisenko, Phys. Lett. B **830**, 137171 (2022), 2205.07239
[13] M. Ablikim et al. (BESIII), Phys. Rev. D **105**, 072002 (2022), 2201.09710
[14] E. Klempt, A.V. Sarantsev, Phys. Lett. B **826**, 136906 (2022), 2112.04348
[15] R. Aaij et al. (LHCb), Phys. Rev. D **90**, 012003 (2014), 1404.5673
[16] R. Aaij et al. (LHCb), Phys. Rev. D **89**, 092006 (2014), 1402.6248
[17] R. Aaij et al. (LHCb), JHEP **08**, 037 (2017), 1704.08217
[18] A. Etkin et al., Phys. Lett. B **201**, 568 (1988)
[19] M. Ablikim et al. (BESIII), Phys. Rev. Lett. **129**, 042001 (2022), 2201.10796